

Transmission Path Analysis of Noise and Vibration in a Rotary Compressor by Statistical Energy Analysis

Seon-Woong Hwang

Digital Appliance Research Lab., LG Electronics, Seoul 153-802, Korea

Weui-Bong Jeong*, Wan-Suk Yoo, Kyu-Hwan Kim

Department of Mechanical Engineering, Pusan National University,

Busan 609-735, Korea

The hermetic rotary compressor is one of the most important components of an air conditioning system since it has a great effect on both the performance and the noise and vibration of the system. Noise and vibration occurs due to gas pulsation during the compression process and to unbalanced dynamic force. In order to reduce noise and vibration, it is necessary to identify their sources and transmission path and effectively control them. Many approaches have been tried in order to identify the noise transmission path of a compressor. However, identification has proven to be difficult since the characteristics of compressor noise are complicated due to the interaction of the compressor parts and gas pulsation. In this study, the statistical energy analysis has been used to trace the energy flow in the compressor and to identify the transmission paths from the noise source to the exterior sound field.

Key Words : Rotary Compressor, SEA, Modal Density, Damping Loss Factor, Coupling Loss Factor, Power Spectrum, Point Mobility

1. Introduction

The hermetic rotary compressor has been widely used for domestic air conditioners. It is one of the most important components of an air conditioning system and it has great effects on the performance and the noise and vibration of the system. Recently, the attenuation of noise and vibration has become more and more important with increasing needs for living amenity. Noise and vibration occurs due to gas pulsation, mass imbalance, electrical force of the motor, and other factors, when the compressor is under operation. Generally, a rotary compressor has high frequency noise and vibration characteristics. However,

it is difficult to make clear the source of noise and vibration because of the coupling effect between fluid flow and structures. A general method to analyze structures, FEM (Finite Element Method), has some limitations over the high frequency band due to limited mesh size and computer memory. If the mesh size is coarse, the accuracy of analysis can be lower. The SEA (Statistical Energy Analysis) is used as an alternative in order to analyze complicated structures having high frequency characteristics. A basic theory of SEA (Lyon, 1975) has been introduced and power flow (Lyon, 1995) between two linear resonator systems was calculated. A coupled system with 3 flat plates (Heckl, 1994) has also been applied. The power flow of a scroll compressor (Rockwood, 2000), a kind of rotary compressor, has been identified using the SEA. Some methods (Kim, 2002) to measure the SEA parameters, modal density and damping loss factor, were compared in the case of a simple beam and flat plate. An added mass effect (Kim, 1999)

* Corresponding Author,

E-mail : wbyeong@pusan.ac.kr

TEL : +82-51-510-2337; FAX : +82-51-517-3805

Department of Mechanical Engineering, Pusan National University, Busan 609-735, Korea. (Manuscript

Received January 13, 2004; Revised July 7, 2004)

in the coupling points of structures has also been studied experimentally, which showed that power flows with difficulty as the added mass to coupling points increases. The SEA has also been applied to the noise analysis of a ship structure (Hyun and Kim, 1996).

In this study, the noise and vibration transmission path and noise radiation of a rolling-piston-type rotary compressor is predicted. Figure 1 shows the simplified SEA model of a rotary compressor. In order to adapt the SEA to a rotary compressor, the SEA parameters, modal density, damping loss factor and coupling loss factor, must be known either analytically or experimentally. Rotary compressor consists of motor and compression parts that have comparatively low modal density and has parts like plate such as shell, accumulator, top cap and bottom cap with higher modal density. The cylinder is connected to the shell inside by point welding as shown in

Fig. 1. Exciting force such as compression force is acted on the cylinder. So the total system of rotary compressor is simplified to 5 main subsystems with high modal density. Input power is excited at the position of 35.9 mm in the z-direction with x, y unit vector. Commercial package AutoSEA 2.3 is used to analyze those systems with the experimental SEA parameters. Acoustic cavity is also considered inside shell and accumulator. The property of acoustic cavity has the speed of sound (=180.4 m/s) and density (=69.4 kg/m³) of refrigerant, R22 at the condition of temperature 100°C and pressure 2.1 Mpa.

According to the results of the analysis, some design parameters were changed to reduce noise, and the predicted results were validated experimentally.

2. Modal Density

Generally, asymptotic modal density formula is available for ideal subsystems such as bar, beam, flat plate, thin-walled cylinder. However, an experimental approach is more suitable for complicated systems such as compressor components. Experimental modal density can be obtained by measuring the point mobility that is commonly referred to as a transfer function of response velocity to an exciting force. Modal density can be defined as following the formula (Lyon, 1995 ; Beranek, 1992)

$$n(\omega) = 4S\rho_s \overline{\text{Re}[Y(\omega)]} \tag{1}$$

where S is the surface area of the test subsystem, ρ_s is the surface mass (mass per unit area), and $\overline{\text{Re}[Y(\omega)]}$ is the space-averaged real part of the mobility. This experimental method was verified with a simple flat plate that has comparatively well known analytical solutions, and then the modal densities of the compressor components were obtained. Figure 2 represents the comparison of the SEA, FEM and experimental results for the flat plate. In the case of the flat plate, there is a good agreement between their results below 4 kHz. However, the FEM results show that it has a limitation in adapting to a high frequency, such as above 4 kHz, due to mesh size. Analytical

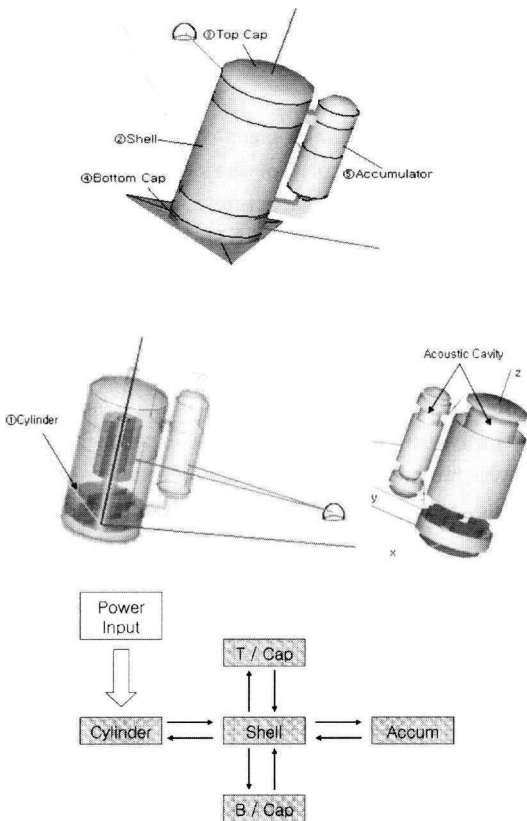


Fig. 1 SEA model of a rotary compressor

solution (Lyon, 1995 ; Beranek, 1992) to the flat plate is given by

$$n(f) = \frac{S\sqrt{12}}{2C_L t}, C_L = \sqrt{\frac{E}{\rho(1-\nu^2)}} \quad (2)$$

where S is the surface area of the flat plate, t is the thickness, E is the longitudinal elastic modulus, ρ is the density and ν is the Poisson's ratio, C_L is the speed of sound of the in-plane compressional wave.

Figure 3 shows the modal density of the compressor shell. The modal density formula of the cylindrical shell (Auto SEA Manual, 2001) is defined as

$$n(f) = \pi \frac{S\sqrt{12}}{2\rho C_L t}, f > f_r$$

$$= \left(\frac{f}{f_r}\right)^{2/3} \frac{S\sqrt{12}}{2C_L t}, f < f_r \quad (3)$$

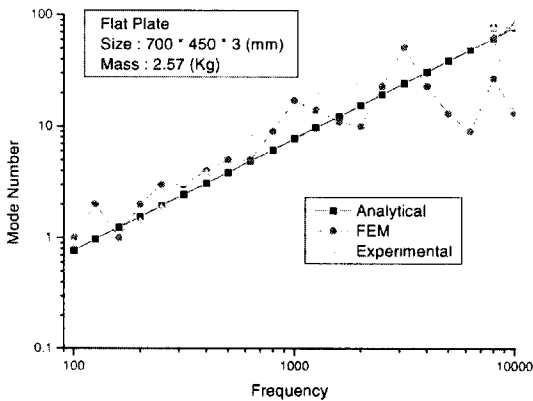


Fig. 2 Modes in band of a simple plate

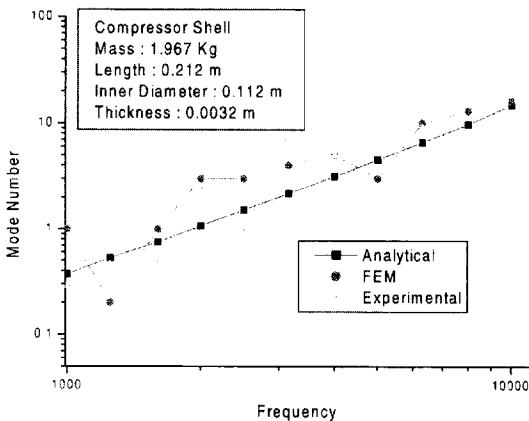


Fig. 3 Modes in band of a shell

where $f_r = \frac{C_L}{2\pi a_m}$ and a_m is the mean radius of the shell. There is comparatively good agreement among the SEA, the FEM and experimental results in the case of the compressor shell.

3. Damping Loss Factor

In general, there are three methods, including the half power bandwidth method, the decay rate method and the power balance method, to determine the damping loss factor of a structure. In this study, power balance method was used to determine the damping loss factors of the compressor components. Damping loss factor η (Lyon and Dejong, 1995) is defined as

$$\eta = \frac{\Pi_{in}}{2\pi f E} = \frac{\text{Re}[F \cdot v]_{in}}{2\pi f M \langle v^2 \rangle} \quad (4)$$

where Π_{in} is the input power, E is the energy of the subsystem expressed by M⟨v²⟩, and M is the mass of subsystem. Each subsystem is excited by impact hammer Type 8203 (B&K) and velocity is obtained by Accelerometer—Type 4393 (B&K). DLF η can be calculated by using the point mobility at the driving points and averaged transfer mobilities. Figure 4 shows the damping loss factors of the compressor components measured with the power balance method. The experiment was performed on a compressor which has a shell size of Φ112 mm, length 212 mm and a cooling capacity of 9,300 Btu/h. Among the compressor components, the cylinder

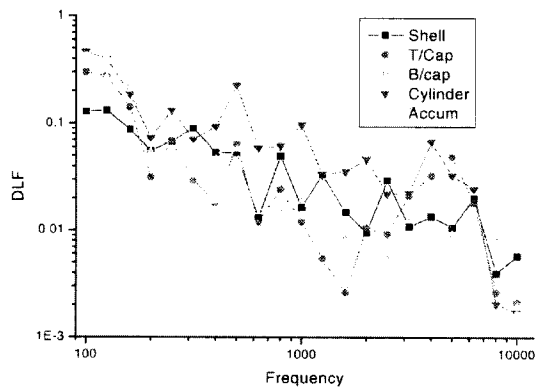


Fig. 4 DLF of compressor parts

had the highest damping value. Its material is gray cast iron.

4. Coupling Loss Factor

The coupling loss factor is a unique concept used in the SEA. It describes the connection between two coupled systems. The coupling loss factor determines the degree of coupling between two subsystems. For the calculation of the coupling loss factor of compressor components, the modal densities, the damping loss factors, and the energies of subsystems are used, and the following formula (Lyon, 1995) is derived from power balance equation :

$$\frac{E_2}{E_1} = \frac{n_2 \eta_{21}}{n_1 \eta_2 + n_1 \eta_{21}} \tag{5}$$

where E_1 , E_2 are the energies of subsystems 1 and 2, n_1 , n_2 are the modal densities of subsystem 1 and 2, and η_1 , η_2 are the damping loss factors of subsystems 1 and 2, respectively. If the reciprocity principle $\eta_{21} = \frac{n_1}{n_2} \eta_{12}$ (Beranek, 1992) is used, the final coupling loss factor between subsystems 1 and 2 can be written as

$$\eta_{12} = \eta_2 \frac{n_2 E_2}{n_2 E_1 - n_1 E_2} = \frac{\eta_2}{\frac{M_1 \langle v_1^2 \rangle}{M_2 \langle v_2^2 \rangle} - \frac{n_1}{n_2}} \tag{6}$$

A preliminary test was performed to determine the coupling loss factor of two L-shaped subsystems which are perpendicularly connected to each other. When a force is applied by impact

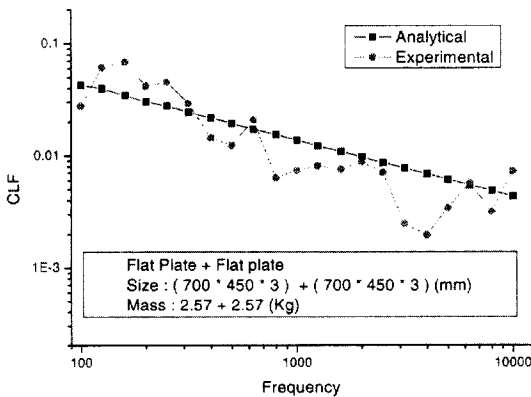


Fig. 5 CLF of perpendicular plates

hammer, the velocity of each system is measured by an accelerometer in order to calculate the subsystem energy. The measured coupling loss factor of a flat plate-plate joint structure is shown in Fig. 5. The analytical solution has a good agreement with the experimental result. The formula (Auto SEA Manual, 2001) to calculate the coupling loss factor of the flat plate-plate joint structure is expressed by

$$\eta_{12} = \frac{2C_B L \tau_{12}}{\pi \omega S_1}, C_B = \sqrt{0.29 C_L t \omega} \tag{7}$$

$$C_L = \sqrt{\frac{E}{\rho(1-\nu^2)}}$$

where L is the connected line length, τ_{12} is the transmission coefficient of the direct coupling of subsystems 1 to 2, ω is the center frequency, S is the surface area of the flat plate, t is the thickness of the flat plate, E is the longitudinal elastic modulus, ρ is the density and ν is the Poisson's ratio, C_B is the sound speed of flexural wave, C_L is the sound speed of in-plane compressional wave.

Figure 6 shows the coupling loss factor between the shell and the cylinder of compressor. Figure 7 shows the coupling loss factor between the shell and the bottom cap. Regrettably, there is no analytical solution for the compressor components. However, it is expected that the result is valid since the result of the flat plate model is valid. Figure 6 illustrates that energy is transmitted better from the cylinder to the shell than in the reverse direction. Figure 7 demonstrates that the energy transfer from the bottom cap to the shell is

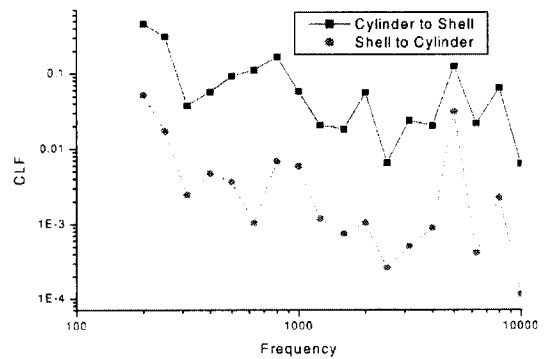


Fig. 6 CLF of a shell-cylinder structure

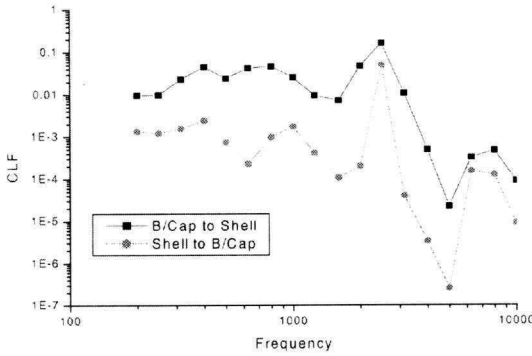


Fig. 7 CLF of shell-B/Cap structure

also easier than in the reverse direction.

5. Energy Distribution and Noise Radiation

A power balance equation for a total system that has a matrix form can be built by using the modal densities, the damping loss factors and the coupling loss factors of compressor components. The energy distribution of the total system to a given power can be calculated by solving the following equation :

$$\omega \eta_i E_i + \omega \sum_{j=1, j \neq i}^m (\eta_{ij} E_i - \eta_{ji} E_j) = \Pi_{i, in} \quad (8)$$

where $\Pi_{i, in}$ is the input power of the external force, E_i is each system's energy, and ω is the center frequency.

Figure 8 shows the noise spectrum of the compressor measured at the position of 30 cm from the compressor shell surface in the x-direction which is perpendicular to accumulator position. It is difficult to measure real input force of rotary compressor due to its complicate exciting mechanism. Therefore, the force 1 N having unit vector in x, y, z directions respectively is assumed intentionally to act on the cylinder. Trial and error shooting method was used to find real input force until the calculated noise spectrum has a good agreement with the experimental one. Figure 9 shows the noise spectrum calculated with the analytical method at the same position when the cylinder is excited by the unit force, 1 N. A commercial package, AutoSEA2, was used to

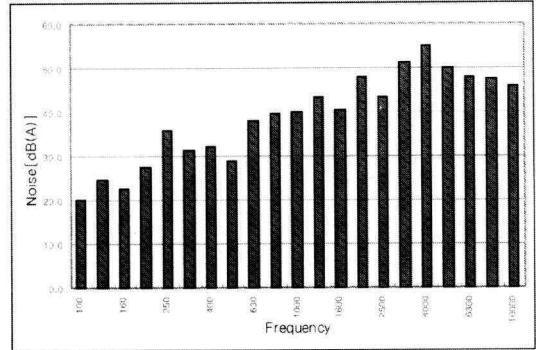


Fig. 8 Radiated Noise of a compressor by experiments

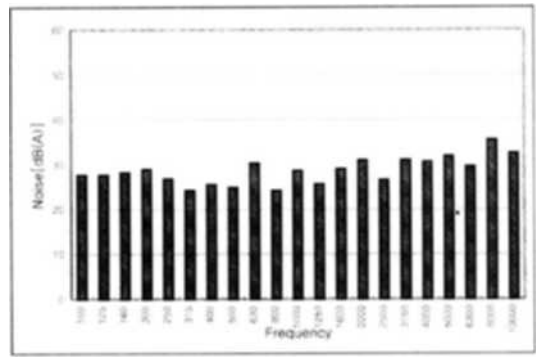


Fig. 9 Radiated noise of a compressor when unit force is applied to a cylinder

calculate the radiation noise from the energy distribution. Sound radiation by vibrating structures such as the plate and the curved shell is dependent on radiation efficiency (Fahy, 1985), which is defined as the ratio of the actual radiation of sound energy compared with that from a plane surface of the same area. Radiation efficiency of the structure, ρ , is defined by the following equation :

$$\Pi = \pi z^2 p_{rms} u_{rms} = \sigma \rho_0 c S \langle \overline{v^2} \rangle \quad (9)$$

where p_{rms} is the root mean square of the radiated pressure at some point in space, u_{rms} is the corresponding root mean square acoustic particle velocity at the same point, z is the radius of the vibrating piston, $\langle \rangle$ indicates the time-average, $\overline{}$ represents the space-average, S is the radiating surface area of the structure, ρ_0 is the density of the fluid medium, and c is the speed of sound in the fluid medium.

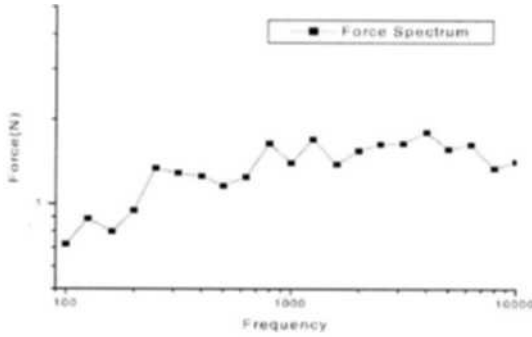


Fig. 10 Spectrum of input force

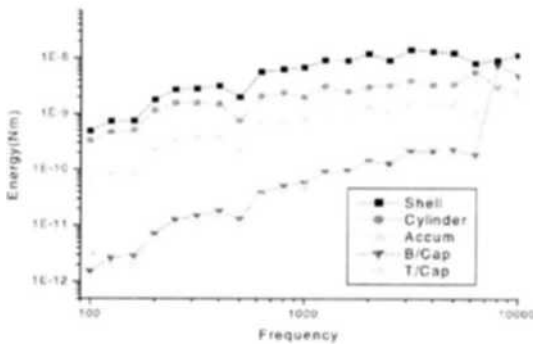


Fig. 11 Energy flow of a base model

The real input force of the compressor is estimated by the comparison of two noise levels, such as Figs. 8 and 9. Figure 10 shows the estimated input force spectrum. Substituting the force spectrum shown in Fig. 10 into eq. (8), the total system energy of the compressor components could be calculated. Figure 11 shows the energies of the subsystems of the rotary compressor. The shell had the largest vibration energy over the all frequencies including 1 kHz and 4 kHz that is the dominant frequencies of general rotary compressor. The cylinder and the accumulator also had an effect on those frequencies. However, most of components had an effect to the noise above 5 kHz.

6. Sensitivity Analysis

Noise Radiation of the compressor occurs due to the structural vibration of each component and the noise level is determined by the vibration energy of the structures. In order to investi-

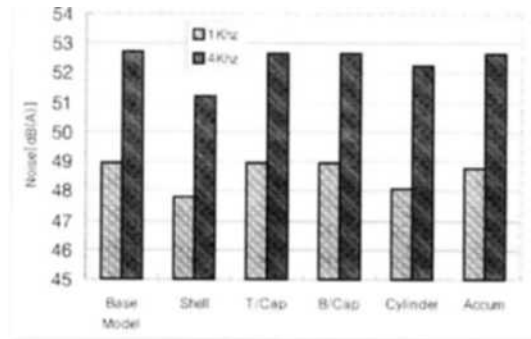


Fig. 12 Radiated noise of a compressor when DLF of each component increases double

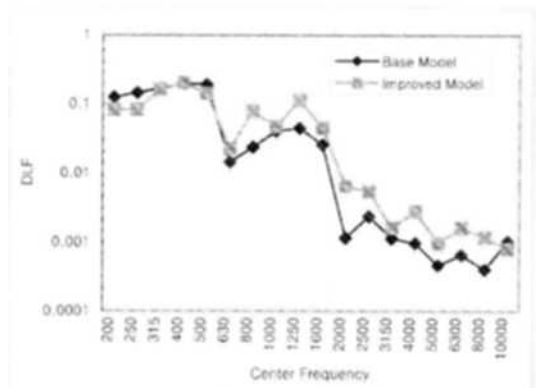


Fig. 13 DLF of the improved model

gate the effects of each subsystem on the radiated noise, the damping loss factors of the compressor components are changed from the experimental value to the 100%-increased value respectively, and the noise level is compared at the 1 kHz and 4 kHz. Fig. 12 shows noise level when each subsystem's DLF was changed. It was found that the vibration energy of the shell has the largest effect on reducing the radiated noise. On the basis of this result, the thickness and length of the bottom cap were increased to increase the damping loss factor and the modified bottom cap was inserted into the shell inside. And then shell was welded to a thicker and longer bottom cap. However, AutoSEA used shorter shell length and longer bottom cap in convenience of analysis. Analysis result using experimental SEA parameters is considered to be valid. Figure 13 shows the comparison of the damping loss factors between the

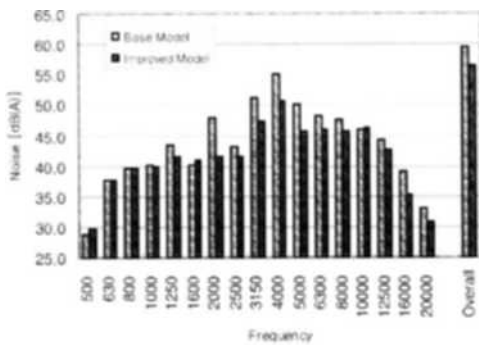


Fig. 14 Radiated noise of the improved compressor by experiments in the x-direction

base model and the improved model. It can be known that the damping loss factor of the modified model increases above the frequency of 1 kHz. Figure 14 represents the noise spectra of the base model and the modified model, respectively. The noise level decreased by about 3dB(A) with the design change. Especially, it was found that the noise of the compressor above the frequency of 1 kHz could be alleviated.

7. Conclusions

The following conclusions were obtained by applying the SEA to the rotary compressor.

- (1) Among the evaluated compressor components, the cylinder has the largest damping loss factor.
- (2) Vibration energy flows easier from the cylinder to the shell than in the reverse direction.
- (3) The effect of the compressor shell vibration is dominant at the 1 kHz and 4 kHz band frequencies.
- (4) Radiation noise can be decreased by changing the shell design using the SEA.
- (5) It is possible to use the SEA as a tool for analyzing the high frequency band noise of a rotary compressor.

Acknowledgment

The authors would like to thank the Ministry of Science and Technology of Korea for the financial support by a grant (M1-0203-00-0017)

under the NRL (National Research Laboratory).

References

- AutoSEA Manual, 2001, SEA Theory and Q & A.
- Beranek, L. L., 1992, Noise and Vibration Control Engineering, *John Wiley & Sons*.
- Clarkson, B. L., 1981, "Experimental Determination of Modal Densities and Loss Factors of Flat Plate and Cylinders," *Journal of Sound and Vibration*, pp. 535~549.
- Fahy, F., 1985, "Sound and Structural Vibration: Radiation, Transmission and Response," Academic Press.
- Heckl, M. and Lewit, M., 1994, "Statistical Energy Analysis as a Tool for Quantifying Sound and Vibration Transmission Paths," *Statistical Energy Analysis: An Overview, with Applications in Structural Dynamics*, Cambridge Univ. Press. pp. 19~34.
- Hyun, M. H. and Kim, S. S., 1996, "A Study on the Transmission Path of Shipboard Structure-Borne Noise Using SEA," *Journal of the Korean society for Noise and Vibration Engineering*, Vol. 6, No. 5, pp. 575~585.
- Kim, K. J. and Choi, S. K., 1999, "Experimental Methods for the measurement of Damping Loss Factors," *Journal of the Korean society for Noise and Vibration Engineering*, Vol. 9, No. 6, pp. 1187~1192.
- Kim, K. J., Kim, J. T., Yoon, T. J. and Park, B. H., 2002, "Added Mass Effect on Structural Junction: Comparison of SEA Experimental Results with Analysis," *2002 Conference of the Korean society for Noise and Vibration Engineering*, pp. 359~364.
- Lyon, R. H. and Dejong, R. G., 1995, *Theory and Application of Statistical Energy Analysis*, Butterworth-Heinemann, Boston.
- Lyon, R. H., 1975, "Statistical Energy Analysis of Dynamic System: Theory and Application," Cambridge, Mass.: MIT Press.
- Rockwood, W. G., 2000, Noise and Vibration Characterization and Statistical Energy Analysis of a Scroll Compressor. 15th Purdue Conf. pp. 331~336.